

# Supporting Information

## Effective trapping of polysulfides using functionalized thin-walled porous carbon nanotubes as sulfur host for lithium-sulfur batteries

Wenhao Liang, Yakun Tang, Lang Liu\*, Caixia Zhu, and Rui Sheng

*Key Laboratory of Energy Materials Chemistry, Ministry of Education; Institute of Applied Chemistry, Xinjiang University, Urumqi 830046, Xinjiang, China.*

**Corresponding author's email:** [liulang@xju.edu.cn](mailto:liulang@xju.edu.cn); [llyhs1973@sina.com](mailto:llyhs1973@sina.com)

The supporting information consists of the following content:

1. The details of materials, materials characterization and electrochemical measurement. Page S-2
2. Figure S1. TEM (a) and HRTEM (b) images of HOCNTs Page S-4
3. Figure S2. SEM images of HCNTs (a, c) and HOCNT (b, d), the corresponding oxygen element mapping images of HCNTs (e) and HOCNTs (f). Page S-4
4. Figure S3. SEM images and EDS patterns of HCNTs (a) and HOCNTs (b). Page S-5
5. Figure S4. Nitrogen adsorption–desorption isotherms (a) and pore size distribution curves (b) of HOCNTs. Page S-5
6. Figure S5. XRD pattern (a) and TG curve (b) of S/BCNT. Page S-6
7. Figure S6. SEM images, corresponding carbon (b, e) and sulfur (c, f) elemental mapping of S/HCNT (a, c, e) and S/HOCNT (b, d, f). Page S-6
8. Figure S7. SEM images of S/BCNT. Page S-7
9. Figure S8. Cycle performance of S/BCNT at 0.2 C. Page S-7

cathodes reported in the literatures.

## **Materials**

Divinyl benzene (80%) (DVB) and boron trifluoride diethyl etherate complex were purchased from Aladdin Reagent Company, and 4-vinylbenzylchlorid (90%) (VBC) was purchased from J&K Chemical Reagent Company. All other reagents were AR grade and provided by commercial suppliers and used without further purification. The synthesis and sulfonation of poly (divinyl benzene) nanotubes (PNTs) are obtained according to the previous reported methods.<sup>1,2</sup>

## **Materials characterization**

X-ray diffraction (XRD, Bruker D8 advance with Cu K $\alpha$  radiation) was used to characterize the phase compositions. Morphologies and structures of products were researched by using field emission scanning electron microscope (FESEM Hitachi S-4800), transmission electron microscope (TEM Hitachi H-600) and a high resolution transmission electron microscope (HRTEM JEOL JEM-2010F). Raman spectra were measured by a Bruker Senterra R200-L spectrometer (532 nm). Bruker VERTEX 70 spectrometer was used to record Fourier transform infrared (FT-IR) spectra. Thermal gravimetric curves (TG, TG-DTA 6200LAB SYS) were used to evaluate the content of sulfur in the S/C composites.

## **Electrochemical measurement**

The electrochemical data were measured with CR2032 button cell, and lithium metal was served as the contrast electrode. 80 wt% active materials, 10 wt% carbon black and 10 wt% poly (vinylidene fluoride) binder were mixed in N-methyl-2-pyrrolidone to form a slurry, which was

smearred on the Al foil and dried at 60 °C for 12 h in vacuum. Cells were assembled in an argon-filled glove box, in which both the moisture and oxygen contents were controlled to be less than 0.1 ppm. Celgard 2400 membrane as the separator. The electrolyte was 1 M lithium bis-(trifluoromethanesulfonyl) imide (LiTFSI) and 1 wt% lithium nitrate (LiNO<sub>3</sub>) in 1,3-dioxolane and 1,2-dimethoxy-ethane (volume ratio 1:1). Galvanostatic charge–discharge tests were carried out by using a Land (CT2001A China) between 1.7 V and 2.8 V (versus Li<sup>+</sup>/Li). Specific capacities were calculated based on the mass of the sulfur.

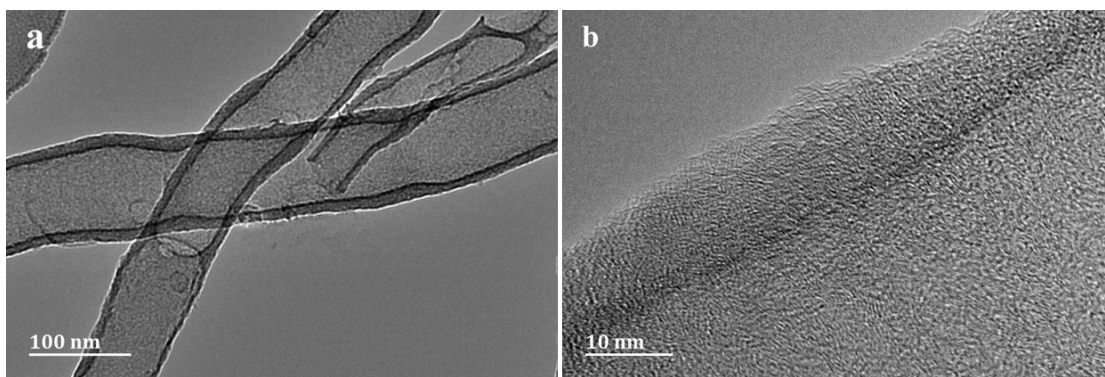
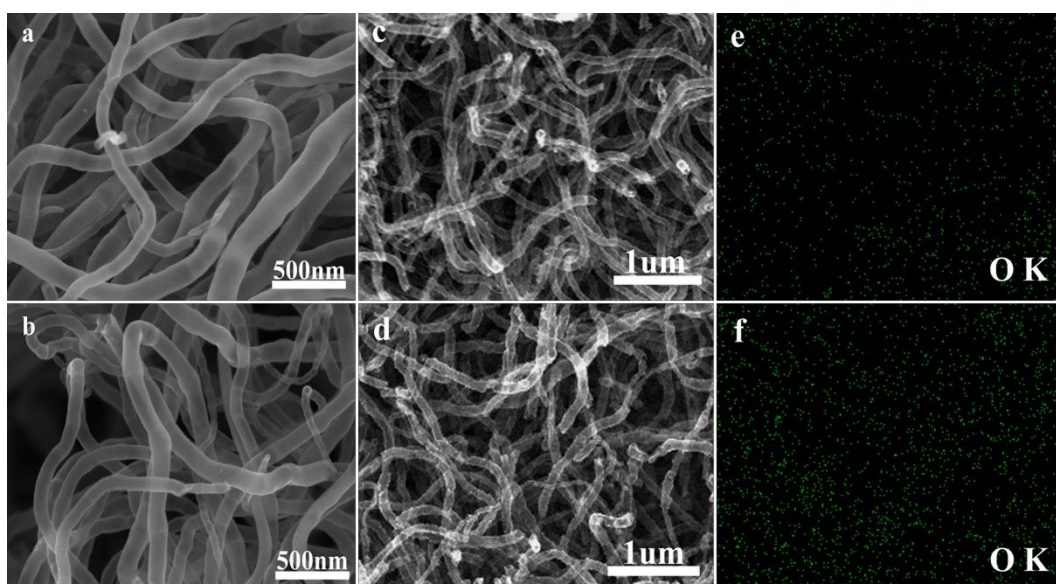
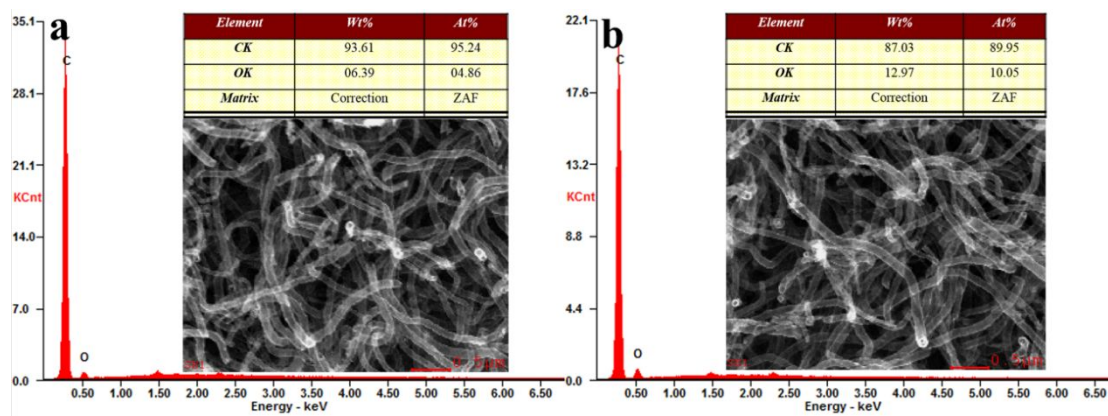


Figure S1. TEM (a) and HRTEM (b) images of HOCNTs.



**Figure S2.** SEM images of HCNTs (a, c) and HOCNTs (b, d), the corresponding oxygen element mapping images of HCNTs (e) and HOCNTs (f).



**Figure S3.** SEM images and EDS patterns of HCNTs (a) and HOCNTs (b).

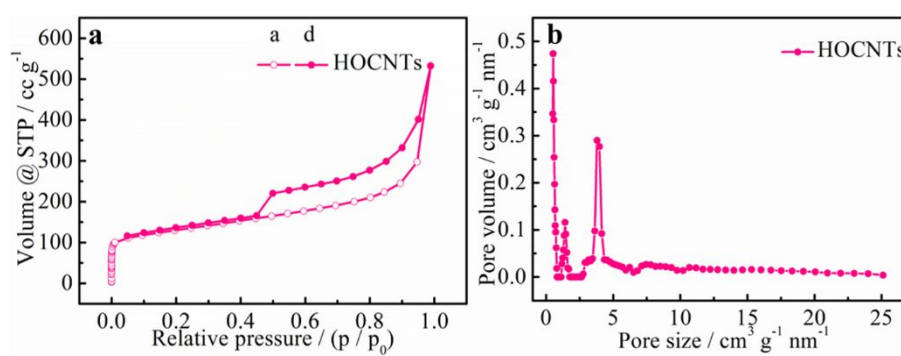


**Figure S4.** Nitrogen adsorption-desorption isotherm (a) and pore size distribution curve (b) of

HOCNTs.

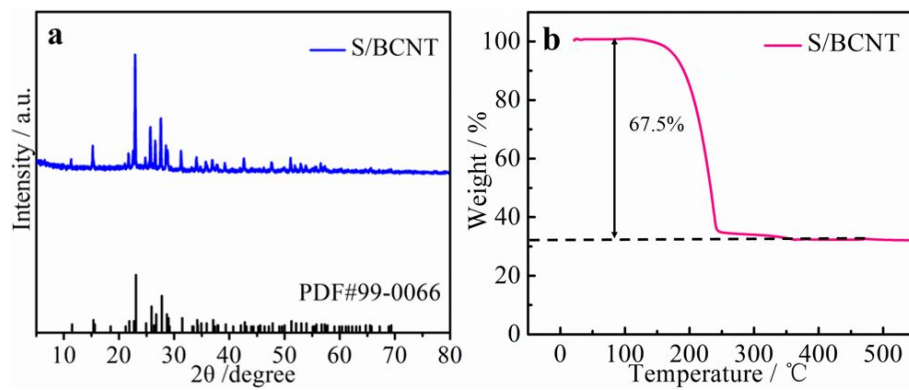


**Figure S5.** XRD pattern (a) and TG curve (b) of S/BCNT.

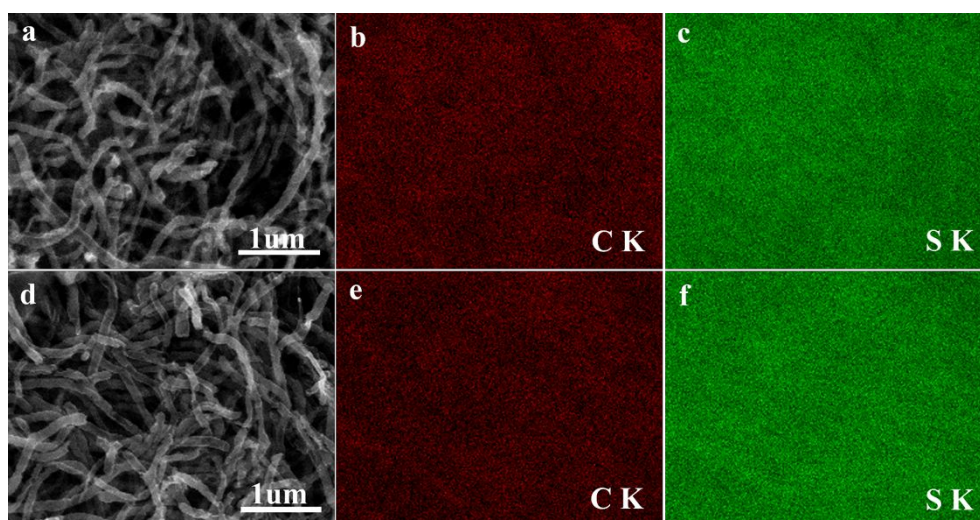


**Figure S6.** SEM images of S/HCNT (a) and S/HOCNT (d), corresponding carbon (b, e) and sulfur (c, f) elemental mapping.

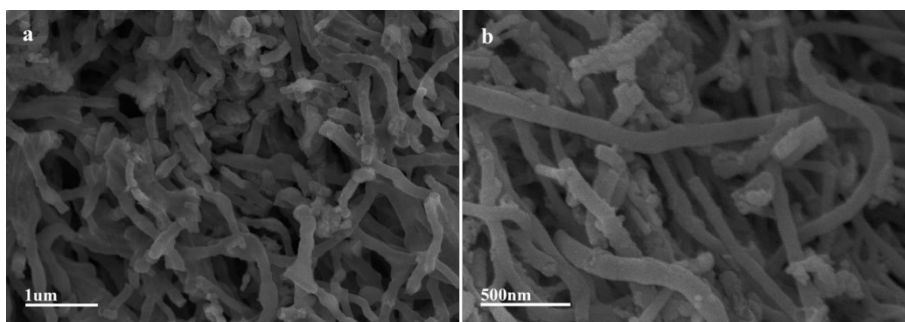


**Figure S7.** SEM images of S/BCNT.

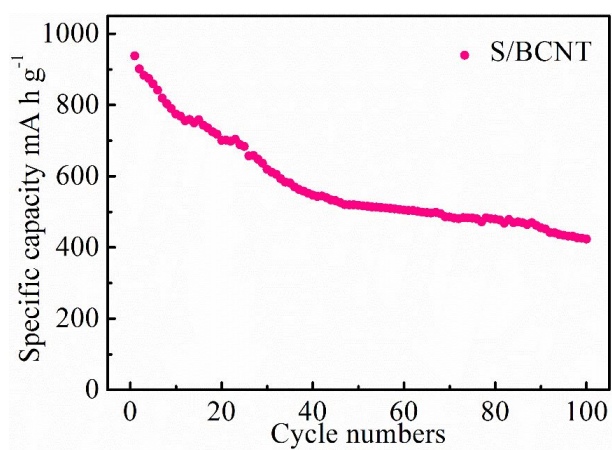


**Figure S8.** Cycle performance of S/BCNT at 0.2 C.

**Table S1.** Cycling performance and specific capacity of various S/CNT cathodes reported in the literature.

| Materials                       | Sulfur % | Current density | Cycle numbers | Remaining capacity (mA h g <sup>-1</sup> ) | Refs |
|---------------------------------|----------|-----------------|---------------|--|------|
| S/Partially Unzipped CNT        | 51%      | 0.2 C           | 60            | 707.2                                      | 3    |
| S/N-doped C@CNT                 | 70%      | 0.2 C           | 100           | 717.6                                      | 4    |
| S/N-doped C/CNT hybrids         | 62.5%    | 1 C             | 600           | 407  | 5    |
| S/acidized CNT paper            | 70%      | 1 C             | 400           | 454  | 6    |
| S/CO <sub>2</sub> oxidation CNT | 80%      | 0.2 C           | 300           | 430.5                                      | 7    |
| S/Polymer/Porous long CNT       | 58%      | 0.5 C           | 200           | 610  | 8    |
| S/HOCNT                         | 70%      | 0.2 C           | 100           | 798.5                                      | This |
|                                 |          | 1 C             | 500           | 511.6                                      | work |

## References

- (1) Ni, W.; Liang, F. X.; Liu, J. G.; Qu, X. Z.; Zhang, C. L.; Li, J. L.; Wang, Q.; Yang, Z. Z., Polymer Nanotubes toward Gelating Organic Chemicals. *Chem. Commun.* **2011**, *47*, 4727-4729.
- (2) Zhou, H. J.; Liu, L.; Wang, X. C.; Liang, F. X.; Bao, S. J.; Lv, D. M.; Tang, Y. K.; Jia, D. Z., Multimodal Porous CNT@TiO<sub>2</sub> Nanocables with Superior Performance in Lithium-Ion Batteries. *J. Mater. Chem. A* **2013**, *1*, 8525-8528.
- (3) Jeong, Y. C.; Lee, K.; Kim, T.; Kim, J. H.; Park, J.; Cho, Y. S.; Yang, S. J.; Park, C. R., Partially Unzipped Carbon Nanotubes for High-Rate and Stable Lithium–Sulfur Batteries. *Journal of Materials Chemistry A* **2016**, *4*, 819-826.
- (4) Zhu, X.; Li, Y.; Li, R.; Tu, K.; Li, J.; Xie, Z.; Lei, J.; Liu, D.; Qu, D., Self-Assembled N-Doped Carbon with a Tube-in-Tube Nanostructure for Lithium-Sulfur Batteries. *J. Colloid Interf. Sci.* **2020**, *559*, 244-253.
- (5) Cai, J.; Wu, C.; Yang, S.; Zhu, Y.; Shen, P. K.; Zhang, K., Templated and Catalytic Fabrication of N-Doped Hierarchical Porous Carbon–Carbon Nanotube Hybrids as Host for Lithium–Sulfur Batteries. *ACS Appl. Mater. Interfaces* **2017**, *9*, 33876-33886.
- (6) Xu, G.; Kushima, A.; Yuan, J.; Dou, H.; Xue, W.; Zhang, X.; Yan, X.; Li, J., Ad Hoc Solid Electrolyte on Acidized Carbon Nanotube Paper Improves Cycle Life of Lithium–Sulfur Batteries. *Energ. Environ. Sci.* **2017**, *10*, 2544-2551.
- (7) Wang, D. T.; Wang, K.; Wu, H. C.; Luo, Y. F.; Sun, L.; Zhao, Y. X.; Wang, J.; Jia, L. J.; Jiang, K. L.; Li, Q. Q.; Fan, S. S.; Wang, J. P., Co<sub>2</sub> Oxidation of Carbon Nanotubes for Lithium-Sulfur Batteries with Improved Electrochemical Performance. *Carbon* **2018**, *132*, 370-379.
- (8) Tiwari, V. K.; Song, H.; Oh, Y.; Jeong, Y., Synthesis of Sulfur-Co-Polymer/Porous Long Carbon Nanotubes Composite Cathode by Chemical and Physical Binding for High Performance Lithium-Sulfur Batteries. *Energy* **2020**, *195*, 117034.